Russian Journal of General Chemistry, Vol. 71, No. 7, 2001, pp. 1109–1115. Translated from Zhurnal Obshchei Khimii, Vol. 71, No. 7, 2001, pp. 1175–1181.

Deprotonation of Synthetic Polyadenyl–Polyuridyl Acid in Aqueous Solution

A. G. Kudrev

St. Petersburg State University, St. Petersburg, Russia

Received January 17, 2000

Abstract — Ultraviolet and circular dichroism spectroscopies were used to examine the acid–base equilibrium of a double-helix synthetic polyadenyl–polyuridyl Poly(A)–Poly(U) acid in neutral and alkaline aqueous solutions. The deprotonation initially has a positive cooperativity which changes for negative at the deprotonation degree $\alpha > 1/2$. A model is proposed, that explains the titration curves and the complex dependence of pK_a on pH for Poly(A)–Poly(U) in going from the neutral to alkaline region. The model is based on the allowance for the effect of immediate environment on the internal protonation constant of ideal polymer.

Studies on the acid–base properties of high-molecular synthetic polynucleotides are important for understanding of the biological activity of the latter *in vivo* [1]. Polyribonucleotides are applied as antitumor drugs [2] and interferon inductors [3, 4]. Double-helix polynucleotides are much more active than single chains. It is assumed that the activity of double-helix polymers is reduced by their disproportionation at high ionic strengths of solutions [3, 4]. In this connection of interest is the behavior of such polymers as various pHs. In the present work as the object for study we used a double-helix synthetic polyadenyl–polyuridyl acid Poly(A)–Poly(U). The role of the acid–base center in Poly(A)–Poly(U) in neutral and alkaline media is played by the uracil N^3 atom. This uracil nitrogen atom comes into composition of natural and synthetic nucleic acids and can be protonated or deprotonated in aqueous solutions, depending on pH [5]. The uracil N^3 atom is involved in H bonds that determine the structure and properties of nucleic acids [6]. Therefore, it is interesting to find out how the acidity of this atom affects H-bond formation in a double-helix polynucleotide compared with a single ribonucleotide chain.

Studies on the acid–base properties of a series of polynucleotides showed that the formally estimated protonation constants of the constituent bases of these polynucleotides depend on the deprotonation degree α [5, 7–10]. The observed $pK_a(\alpha)$ dependences were qualitatively explained by the polyelectrolyte effect and conformational changes in the course of protonation–deprotonation. The concentration profiles in [7–10] were constructed using chemometric procedures based on the factor analysis. A feature of the factor analysis is that the calculations require no postulated chemical model of the system, but, as a consequence, the resulting profiles are purely analytical and can only be interpreted on a qualitative level. The present work was aimed at constructing a mathematical model that would impart a physicochemical sence to the profiles obtained by the factor analysis of spectrophotometric titration data for solutions containing polynucleotides. By the least-squares treatment of experimental titration data for solutions of macromolecules one can obtain parameters for a specific chemical model of the equilibrium. However, the use of this method is complicated by the intricate problem of constructing the mass balance equation complying with the mass action law [11]. Binding constants for polymers with regularly repeated structural units as binding centers are most commonly estimated by the Scatchard method [12]. The improved Scatchard method takes account of the cooperativity of polymer saturation with ligand [13].

Relation of polymer intrinsic constant to formation function. The stability constant of a complex formed by an ideal polymer $PolyX_k$ can, from statistical considerations [14, 15], be written as follows.

$$B'_k = \frac{N(N-1)(N-2)...(N-k+1)\bar{K}^k}{k!}. \qquad (1)$$

Here $\bar{K} = (B'_N)^{1/N}$ is the internal constant measuring the ability of a polymer Poly to add a ligand X; N is the number of monomers in the chain; and k is the number of added ligands. The sum of the formation constants of all $PolyX_k$ complexes is a Macloren power series in the intrinsic constant.

1070-3632/01/7107-1109 $25.00

$$1 + \sum^{N} B'_k = (1 + \bar{K})^N. \quad (2)$$

As follows from Eq. (2), for an ideal polymer solution, the total component concentrations are obviously related to the intrinsic constant.

$$C_{\mathrm{Mon}} = [\mathrm{Mon}](1 + \sum^{N} B'_k[\mathrm{X}]^k) = [\mathrm{Mon}](1 + \bar{K}[\mathrm{X}])^N, \quad (3)$$

$$C_{\mathrm{X}} = [\mathrm{X}] + \frac{[\mathrm{Mon}]}{N} \sum^{N} kB'_k[\mathrm{X}]^k$$

$$= [\mathrm{X}] + \frac{\bar{K}[\mathrm{X}][\mathrm{Mon}]}{N} (1 + \bar{K}[\mathrm{X}])^{N-1}. \quad (4)$$

Here C_{Mon} and C_{X} are the total concentrations of the monomer and the ligand and [Mon] and [X] are the corresponding equilibrium concentrations. Substituting Eq. (3) into Eq. (4) we obtain Eq. (5) for the formation function. The resulting equation relates experimentally determined concentrations with the intrinsic constant for ideal polymer.

$$\bar{n}_{\mathrm{id}} = \frac{C_{\mathrm{X}} - [\mathrm{X}]}{C_{\mathrm{Mon}}} = \frac{\bar{K}[\mathrm{X}]}{1 + \bar{K}[\mathrm{X}]}. \quad (5)$$

Equation (5) is equivalent to the Scatchard equation for a monodentate ligand. Let us rewrite this equation in the logarithmic form for the protonation process.

$$\mathrm{p}\bar{K}_{\mathrm{a}} = \log\left(\frac{\bar{n}_{\mathrm{id}}}{1 - \bar{n}_{\mathrm{id}}}\right) + \mathrm{pH}. \quad (6)$$

The $\mathrm{p}\bar{K}_{\mathrm{a}}$ value for ideal polymer is a constant that is independent both on the number of monomers in the chain and on the degree of polymer saturation with ligand. With polynucleotides, the experimental dependences for measured physical parameters generally strongly deviate from those predicted for ideal polymer. Linear deviations are interpreted in terms of the polyelectrolyte theory [16] which predicts a linear dependence of $\mathrm{p}\bar{K}_{\mathrm{a}}$ on pH. Nonlinear deviations are interpreted in terms of the Hill cooperativity theory [17]. The cooperativity of interaction can be accounted for by the modernization of the Scatchard method by introduction of the cooperativity factor ω [13]. The physical sence of ω is that the constant of ligand binding into a position neighboring to that occupied by monomer is $\bar{K}\omega$ and into a position between those occupied by monomers, $\bar{K}\omega^2$. With allowance for the cooperativity and in agreement with [13], Eq. (5) takes form (7).

$$n_{\mathrm{c}} = K[\mathrm{X}](1 - mn_{\mathrm{c}}) \left(\frac{(2\omega - 1)(1 - m\bar{n}_{\mathrm{c}}) + \bar{n}_{\mathrm{c}} - R}{(2\omega - 1)(1 - m\bar{n}_{\mathrm{c}})}\right)^{m-1}$$

$$\times \left(\frac{1 - (m + 1)\bar{n}_{\mathrm{c}} + R}{2(1 - m\bar{n}_{\mathrm{c}})}\right)^2. \quad (7)$$

Here $R = \{[1 - (m + 1)\bar{n}_{\mathrm{c}}]^2 + 4\omega\bar{n}_{\mathrm{c}}(1 - m\bar{n}_{\mathrm{c}})\}^{1/2}$, and m is the number of ligated bases. The shape of the profile described by this equation is determined by one type of cooperativity. But, as noted in [7–10], protonation of polynucleotides is accompanied by the polyelectrolyte effect, stacking, and conformational changes. Combined interactions result is that α values control not only the value but also the sign of cooperativity. At fixed m, the region of negative cooperativity can be described separately, by introducing a linear term in Eq. (7) [16]. To fit the entire titration curve by a single equation at a fixed m, in the present work we used the matrix method [18, 19]. The physical model is based on the allowance for interactions between nearest neighbors in a polymer containing a regularly repeated functional group capable of reversibly binding ligands.

Ligands in complex PolyX_k can bind with various monomers, and the number of possible combinations is equal to the number of combinations of k in N (S_k^N). The stability constant B_k of complex PolyX_k is a sum of S_k^N stability constants of separate configurations (chain states) β_i. To find β_i, let us introduce a configurational matrix $\boldsymbol{M}(N, 2^N)$. The configurational matrix $\boldsymbol{M}$ is, in essence, a set of 2^N binary digits. The matrix row M_i represents the possible configuration of a polymer with a sequence of zeroes in positions where monomers are free and with a sequence of units in positions where monomer is bound with ligand. The stability constant of the configuration formed by complex PolyX_k can be represented as follows:

$$\beta_i = \prod_{j=1}^{N} (M_{ij}\bar{K}\omega_j)M_{ij} \neq 0. \quad (8)$$

The correction for mutual effect ω_j was included in the following way: for j from 1 to N, if $M_{ij} \equiv 1$ and $M_{ij+1} \equiv 1$, then $\omega_j^* = 1 - \omega_P$ and $\omega_{j+1}^* = 1 - \omega_P$, and for j from 1 to N, if $M_{ij} \equiv 1$ and $M_{ij+1} \equiv 1$, then $\omega_j = \omega_j^*\omega_H$ and $\omega_{j+1} = \omega_{j+1}^*\omega_H$, where ω_P is a coefficient relating to negative cooperativity, and $\omega \equiv \omega_H$, to positive cooperativity. For ideal polymer including no neighbor effects, $\omega_H = 1$, $\omega_P = 0$, and, consequently, $B_k = B'_k$.

With account for the definition of configurational stability constant, the formation function can be transformed into the matrix form.

$$\bar{n} = \frac{[\mathrm{X}]^{\boldsymbol{S}} \times \boldsymbol{SB_P}}{N(1 + [\mathrm{X}]^{\boldsymbol{S}}\boldsymbol{B_P}}. \quad (9)$$

Here $\boldsymbol{S} = \sum^{N} \boldsymbol{M}$, × is the sign of elementwise matrix multiplication, and $\boldsymbol{B_P}$ is the vector of stability constants with elements β_i. As seen from Eqs. (8) and (9),

$\bar{n}$ depends on the polymer length N, the equilibrium ligand concentration [X], and three independent variables $\bar{K}$, ω_P, and ω_H. When α tends to 1, $\bar{n} \longrightarrow \bar{n}_{id}$, i.e. Eq. (9) gives the same as Eq. (5). Equation (9) allows calculation of the formation function determined by the vector $\boldsymbol{B_P}$. The required parameters $\bar{K}$, ω_H, and ω_P are not correlated and can be correctly calculated by a standard least-square method. In the present work we used a Levenberg–Marquardt version of this method [20]. In tests, the right convergence was observed over a wide range of initial approximations for all the three parameters.

Calculation of concentration profiles from the data matrix. According to the Bouguer–Lambert–Beer law in the matrix form, the experimental absorbance matrix $\boldsymbol{A}(Np, Nw)$ (Np is the number of experimental points and Nw is the number of experimental wavelengths) is a product of a molar absorptivity matrix $\boldsymbol{E}(R, Nw)$ (R is the total number of spectral forms) and a concentration matrix $\boldsymbol{C}(Np, R)$.

$$\boldsymbol{A} = \boldsymbol{CE}. \quad (10)$$

The aim of the factor analysis is to find from the experimetal absorbance matrix the concentration matrix and the molar absorptivity matrix. To this end, one should first of all determine the number of principal factors, which is equal to the number of equilibrium forms whose interconversions give rise to absorbance dispersion. The singular diagonalization procedure allows reproduction of the ith matrix with use of a fixed number of new variables which are a linear combination of initial variables and give the total dispersion.

$$\boldsymbol{A}_i = \boldsymbol{USV}^{\mathrm{T}} + \tau_i = \boldsymbol{A}_i^* + \tau_i \quad (11)$$

Here $\boldsymbol{U}$ and $\boldsymbol{V}^{\mathrm{T}}$ are orthogonal matrices, $\boldsymbol{S}$ is a diagonal matrix in which the number of nonzero diagonal elements is equal to the rank of the matrix $\boldsymbol{A}_i$ (the number of principal factors), $\boldsymbol{A}_i^*$ is the matrix $\boldsymbol{A}_i$ recovered via R factors, and τ_i is the recovered error. The number of principal factors is chosen so that the recovered error τ_i is lower or equal the experimental error. In the present work R values were calculated by the principal component method [21, 22]. To transform the virtual factors calculated by Eq. (11) into factors having a physicochemical sence, one should perform appropriate rotation in the vector space. When there is selectivity in the system, the matrix $\boldsymbol{V}^{\mathrm{T}}$ is related to the matrix $\boldsymbol{E}_i$ of R of the least correlated rows of the matrix $\boldsymbol{A}$, which can be calculated according to [23]. Similarly, the matrix $\boldsymbol{US}$ is transformed into $\boldsymbol{C}_i$. The latter allows recovered, within the experimental error, of the initial data matrix by Eq. (10). Let us write the above-described calculation of the concentration profile as the matrix division operator.

$$\boldsymbol{C}_i = \boldsymbol{A}_i/\boldsymbol{E}_i. \quad (12)$$

Similarly, for the molar absorptivity matrices we can write the matrix division operator.

$$\boldsymbol{E}_i = \{\boldsymbol{A}_i^{\mathrm{T}}/\boldsymbol{C}_i^{\mathrm{T}}\}^{\mathrm{T}} \quad (13)$$

By alternately applying operators (12) and (13) one can calculate optimal, in terms of the least-squares method, values of $\boldsymbol{S}_i$ and $\boldsymbol{E}_i$. Such optimization is called the alternating least-squares (ALS) method. This method provides the best fit to true profiles for systems with concentration or spectral selectivity [24, 25]. However, the ALS method is also suitable when incomplete selectivity takes place. In this case, calculated concentration profiles are fit to true ones via imposition of the so-called "soft" [25–28] (unimodality of concentration profiles $\boldsymbol{C}_i$, non-negativity of $\boldsymbol{C}_i$ and $\boldsymbol{E}_i$, etc.) or "hard" restrictions on the mass balance equations with compliance for the mass action law [29–31]. Correct application of the above restriction allows one to lift the rotational uncertainty characteristic of the factor analysis, and, when the experimental error fits the normal law, the calculated sets of $\boldsymbol{C}_i$ and $\boldsymbol{E}_i$ are normally distributed sets with mathematical expectations of $\boldsymbol{C}$ and $\boldsymbol{E}$, respectively.

The goodness of fit of calculated matrices to experimental ones was evaluated in the present work by the Hamilton factor [32]. Taking account of the uniformity of the absorbance dispersions are all the wavelengths, the weight factors in the Hamilton equation were ignored. Expressing the Hamilton factor in percent and ignoring the weight factors, the goodness-of-fit criterion PE.

$$\boldsymbol{PE}(\boldsymbol{Z}, \boldsymbol{Z}^*) = \left[\frac{\boldsymbol{Tr}\{(\boldsymbol{Z}^* - \boldsymbol{Z})(\boldsymbol{Z}^* - \boldsymbol{Z})^{\mathrm{T}}\}}{\boldsymbol{Tr}\{\boldsymbol{ZZ}^{\mathrm{T}}\}}\right] \times 100\%. \quad (14)$$

Here $\boldsymbol{Z}$ is a matrix to be compared with, $\boldsymbol{Z}^*$ is the calculated marix, and $\boldsymbol{Tr}$ is the matrix trace.

Titration of Poly(A)–Poly(U) by UV absorption data. Absorption matrix $\boldsymbol{A_{UV}}$(45,131). Three titrations of aqueous Poly(A)–Poly(U) with concentrated alkali were performed. After addition of each successive aliquote, the absorption spectrum in the range 220–350 nm at 131 wavelengths was measured. As a result, an experimental absorbance matrix $\boldsymbol{A_{UV}}$(45,131) was formed. By the principal component method we found that the optical density dispersion in $\boldsymbol{A_{UV}}$ is determined by two factors. The model based on the

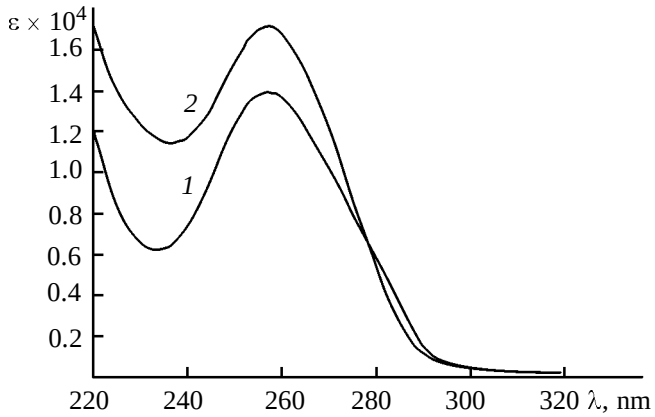

Fig. 1. UV spectra of the (*1*) neutral and (*2*) deprotonated forms of Poly(A)–Poly(U), calculated from the spectral matrix $\boldsymbol{A_{UV}}$ by Eq. (13) and optimized by the ALS method.

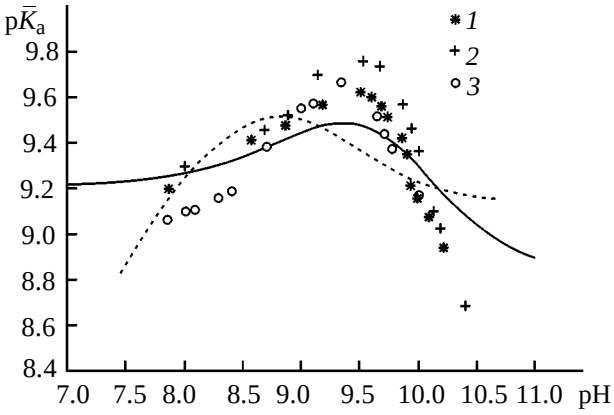

Fig. 2. Experimental dependence of $p\bar{K}_a$ on pH for Poly(A)–Poly(U), calculated by substitution in Eq. (6) of the results of matrix division (16). $C_{Mon} \times 10^5$, M: (*1*) 7, (*2*) 5.2, and (*3*) 6. (Solid line) Theoretical dependence calculated by Eq. (9) ($\bar{K}$ 4.2×10^8, ω_H 12.5, and ω_P 0.48) and (dotted line) theoretical dependence calculated by Eq. (7) ($\bar{K}$ 1.3×10^9, ω 1.93, and m 1.04).

two principal components describes 99.92% of the total dispersion (the rank of the matrix $\boldsymbol{A_{UV}}$ is equal to two).

The optical density dispersion in each titration, too, is determined by two factors. Therefore, in agreement with the Bouguer–Lambert–Beer and with account for Eqs. (3) and (4), for the absorbance in each experimental point at each wavelength, we have Eq. (15):

$$Abs - \varepsilon_X[X] = A_{Mon}(1 - \bar{n}) + A_{MonX}\bar{n}. \quad (15)$$

Here $A_{Mon} = \varepsilon_{Mon}/C_{Mon}$ is the absorbance of the solution in the absence of ligand X (produced by absorption of uncomplexed monomeric units of the polymer, and $A_{MonX} = \varepsilon_{MonX}/C_{Mon}$ is the absorbance of the solution with excess ligand X (produced by absorption of complexed monomeric units of the polymer). Because of the correspondence between Eq. (10) and Eq. (15) the matrix division operator can be applied in the following form:

$$[\bar{\boldsymbol{n}};\ 1 - \bar{\boldsymbol{n}}] = (\boldsymbol{A_{UV}} - \varepsilon_X[X])/[\boldsymbol{A}_{Mon};\ \boldsymbol{A}_{MonX}]. \quad (16)$$

Here the matrix with the elements $1 - \bar{n}$ and $\bar{n}$ can be obtained by division of the experimental absorbance matrix (corrected for the absorbance of uncomplexed ligand $\varepsilon_X[X]$) by the matrix with the elements A_{Mon} and A_{MonX} for all wavelenghs. Knowing the vector $\bar{\boldsymbol{n}}$, one can calculate the logarithmic function of the intrinsic protonation function by Eq. (6). This function is more descriptive of specific features of polymer deprotonation.

The electronic spectra of the protonated and deprotonated forms of Poly(A)–Poly(U) and the $p\bar{K}_a$ values at various pHs, calculated from the experimental spectral matrix $\boldsymbol{A_{UV}}$, are shown in Figs. 1 and 2, respectively.

As seen from Fig. 1, deprotonation is accompanied by growing absorbance at 260 nm, i.e. by disappearance of hypochromism. This fact suggests that the shape of the Poly(A)–Poly(U) molecule changes from a rod-extended double helix in neutral aqueous solution [6] to statistical ball in alkaline solution. Moreover, the theory of the helix–ball transition predicts that even when the hypochromic effect is no longer observed the helix chains are not separated [33]. When it comes to a homopolymer helix, such as Poly(A)–Poly(U), than after most units of one chain has separated from the complementary units of the other chain, fluctuations of some unseparated units are still possible. This is enough for the helix chains not to separate and to continue to move in the medium as a single kinetic unit [34]. In view of the aforesaid, in constructing the model of the acid–base behavior we assumed that Poly(A)–Poly(U), regardless of the conformation, is a single molecule.

As seen from Fig. 2, Poly(A)–Poly(U) differs in behavior from ideal polymer where neighboring pairs of bases are protonated independently of one another. At small α values, $p\bar{K}_a$ increases with increasing pH, on account of the polyelectrolyte effect. In the case in hand, the polyelectrolyte effect increases the intrinsic protonation constant by electrostatic attraction of

proton to bases with deprotonated uracil N^3 atom. The $p\bar{K}_a$(pH) function passes through a maximum, and at $\alpha > 1/2$ a sharp decrease in $p\bar{K}_a$ is observed. The simplest qualitative explanation for the destabilization at high α values is that the cooperativity of H-bond formation prevails over the polyelectrolyte effect. It is known that the total energy of H-bond complex formation between polynucleotide chains is higher that the total energy of pair interactions [6].

Applying Eq. (7) to the whole experimental data set one obtains a cooperativity factor of about two (see table); therewith, the polyelectrolyte effect shows up in that the average number of protonated bases (m) is higher than one.

If the formation function is calculated using operator (16) and then the parameters $\bar{\boldsymbol{n}}$ are calculated by the least-squares method using Eq. (9), then the resulting $p\bar{K}_a$(pH) dependence better fits the experiment than that obtained using Eq. (7). For the model compound for calculations by Eq. (9) we took a cyclic oligomer (N = 8). The cyclic oligomer and endless polymer have almost the same formation functions. For cyclic oligomers with $N > 7$, the dependence of the formation function on the number of chain units can be neglected, unlike the experimental error in the determination of this function. Thus, the difference between the model functions (Np = 100), calculated by Eq. (7) ($p\bar{K}_a$ = 0, ω = 4, and m = 1) for endless polymer and by Eq. (9) ($p\bar{K}_a$ = 0, N = 8, ω_H = 2, and ω_P = 0) for the cyclic polymer, was $PE(\bar{\boldsymbol{n}}_C, \bar{\boldsymbol{n}}) = 3 \times 10^{-3}$%. The Poly(A)–Poly(U) acid studied in the present work is a high-molecular or an endless polymer. The cooperativity parameters calculated for the whole experimental data set by Eq. (9) are listed in the table. Note that the intrinsic constant calculated by this model is slightly lower than that obtained by Eq. (7) or of that commonly used as estimate under the ideal polymer assumption ($p\bar{K}_a$ = pH at $\bar{n}$ = 1/2). The deviation from ideality is accounted for by a high positive cooperativity ω_H of protonation at α values close to 1. At lower α, when electrostatic effects are weakened (all bases pass into the neutral form), negative cooperativity ω_P gets prevailing giving rise to descending $p\bar{K}_a$(pH) function at $\alpha < 1/2$.

Titration of Poly(A)–Poly(U) by curcular dichroism data. Spectral matrix $\boldsymbol{A_{CD}}$(9,131). Nine circular dichroism spectra at various pH were measured, which were used to construct a spectral matrix $\boldsymbol{A_{CD}}$. The least correlated spectra at the lowest and highest pHs were used as initial approximation for the calculation by operators (12) and (13) of the ALS-optimized profile of the formation function and of the spectra of the protonated and deprotonated forms of Poly(A)–Poly(U). The $p\bar{K}_a$(pH) dependence [Eq. (6)] and the cirsular dichroism spectra of the above forms are shown in Figs. 3a and 3b. It can be noted that the $p\bar{K}_a$(pH) function has the same shape as that calculated by absorbance data.

Cooperativity parameters for protonation of Poly(A)–Poly(U), calculated from the experimental absorbance matrix $\boldsymbol{A_{UV}}$ by the factor analysis and the least-squares method

Parameter calculated by the least-squares method[a]	Eq. (7)[b]	Eq. (9)[c]
K[d]	$1.3–10^9$	$(4.2 \pm 0.8)–10^8$
$\omega^{1/2} \equiv \omega_H$[e]	1.93	12.5 ± 3
ω_P[f]	–	0.48 ± 0.03
m[g]	1.04	–
$PE(\bar{n}_{exp} - \bar{n}_{calc})$[h]	2.3	1.7

[a] The errors in parameters were determined by three independent titrations at a confidence probability of 0.05. [b] Optimal parameters for endless polymer, calculated by Eq. (7). [c] Optimal parameters for the cyclic oligomer (N = 8), calculated by Eq. (9). [d] Internal constant. [e] Positive cooperativity. [f] Negative cooperativity (anticooperativity). [g] Mean number of ligated bases. [h] Differences [see Eq. (14)] between the formation constants calculated by the factor analysis by Eq. (14) from experimental data and optimized by the ALS method ($\bar{n}_{exp}$), and the theoretical values ($\bar{n}_{calc}$) obtained by Eqs. (7) and (9).

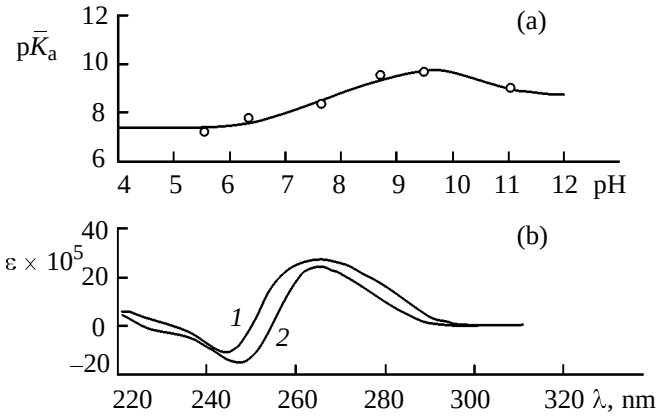

Fig. 3. Results of diagonalization of the spectral matrix $\boldsymbol{A_{CD}}$: (a) $p\bar{K}_a$(pH) dependence; (circles) experimental points, C_{Mon} 6×10^{-5} M; and (b) circular dichroism spectra of the (*1*) neutral and (*2*) deprotonated forms of Poly(A)–Poly(U), calculated by Eq. (13) and optimized by the ALS method.

The change in the circular dichroism spectrum in going from the neutral and alkaline region suggests a change in the conformation of the polymer, providing evidence for the assumption that the macromolecule passes into the statistical-ball state on deprotonation.

EXPERIMENTAL

Synthetic Poly(A)–Poly(U) (Sigma), NaCl (Merck), NaOH (Merck), and HCl (Merck) were used as received. All solutions were prepared with distilled water free of CO_2.

The UV absorption spectra were measured on a Perkin–Elmer Lambda-19 spectrophotometer combined with a personal computer. The temperature (37°C) in the spectrophotometric cell was maintained with a device which utilizes the Peltier effect. Titration and pH measurements were performed in a temperature-controlled cell at 37°C in 0.15 M aqueous NaCl under N_2. The solution in the cell, after addition of a further portion of alkali and measuring pH, was pumped over into a hermetic spectrophotometric cell by means of a peristaltic pump under air-proof conditions. The circular dichroism spectra were measured on a Jasco-720 spectropolarimeter in a temperature-controlled cell at 37°C. pH measurements were performed on an Orion-701A pH-meter.

The theoretical part of this work was financially supported by the Competitive Center for Basic Natural Science at the St. Petersburg State University [grant no. 9-373 (1997)].

REFERENCES

1. Saenger, W., *Principles of Nucleic Acid Structure*, New York: Springer, 1984.
2. Heider, A.R. and Bardos, T.J., *Cancer Chemotherapeutic Agents*, William, O.F., Ed., Washington: ACS Prof. Ref. Book, 1995, p. 529.
3. Blake, R.D., Massoulie, J., and Fresco, J.R., *J. Mol. Biol.*, 1967, vol. 30, no. 2, pp. 291–308.
4. Massoulie, J., *Eur. J. Biochem.*, 1968, vol. 3, no. 4, pp. 439–447.
5. Casassas, E., Gargallo, R., Gimenez, I., Izquierdo-Ridorsa, A., and Tauler, R., *Anal. Chim. Acta*, 1993, vol. 283, pp. 538–547.
6. Jeffery, G.A. and Saenger, W., *Hydrogen Bonding in Biological Structures*, Berlin: Springer, 1994.
7. Izquierdo-Ridorsa, A., Casassas, E., Gargallo, R., Marques, I., and Tauler, R., *React. Funct. Polym.*, 1996, vol. 28, no. 2, pp. 127–137.
8. Casassas, E., Tauler, R., and Marques, I., *Macromolecules*, 1994, vol. 27, no. 7, pp. 1729–1737.
9. Tauler, R., Izquierdo-Ridorsa, A., Gargallo, R., and Casassas, E., *Chemom. Intel. Lab. Systems*, 1995, vol. 27, pp. 163–175.
10. Casassas, E., Gargallo, R., Izquierdo-Ridorsa, A., and Tauler, R., *React. Funct. Polym.*, 1995, vol. 27, no. 1, pp. 1–11.
11. Gargallo, R., Tauler, R., and Izquierdo-Ridorsa, A., *Anal. Chim. Acta*, 1996, vol. 331, no. 3, pp. 195–205.
12. Scatchard, G., *Ann. N. Y. Acad. Sci.*, 1949, vol. 51, pp. 660–662.
13. McGhee, J.D. and Hippel, P.H. von, *J. Mol. Biol.*, 1974, vol. 86, no. 2, pp. 469–489.
14. Gill, S.J., *Biochemical Thermodynamics*, Jones, M.N., Ed., Amsterdam: Elsevier, 1979, pp. 224–264.
15. Hartley, F.R., Burgess, C., and Alcock, R.M., *Solution Equilibria*, Chichester: Horwood, 1980.
16. Friedman, R.A.G. and Manning, G.S., *Biopolymers*, 1984, vol. 23, no. 12, pp. 2671–2714.
17. Hill, T.L., *Cooperativity Theory in Biochemistry. Steady State and Equilibrium Systems*, New York: Springer, 1985.
18. Crothers, D.M., *Biopolymers*, 1968, vol. 6, no. 4, pp. 575–584.
19. Zimm, B.H. and Bragg, J.K., *J. Chem. Phys.*, 1959, vol. 31, no. 2, pp. 526–535.
20. More, J.J., *The Levenberg-Marquardt Algorithm: Implementation and Theory. Numerical Analysis. Lecture Notes in Mathematics 630*, Watson, G.A, Ed., New York: Springer, 1977, pp. 105–125.
21. Malinowsky, E.R. and Howery, D.G., *Factor Analysis in Chemistry*, New York: Wiley, 1980.
22. Llinas, J.R. and Rouis, J.M., *Computer Aids in Chemistry*, Vernin, G, and Chanon, M., Eds., Chichester: Horwood, 1986. Translated under the title *EVM pomogaet khimii*, Moscow: Khimiya, 1990, pp. 182–237.
23. Windig, W. and Guilment, J., *Anal. Chem.*, 1991, vol. 63, no. 14, pp. 1425–1432.
24. Mane, R., *Chemom. Intel. Lab. Systems*, 1995, pp. 89–99.
25. Tauler, R., Smilde, A., and Kowalski, B., *J. Chemometrics*, 1995, vol. 9, no. 1, pp. 31–58.
26. Tauler, R. and Casassas, E., *Analusis*, 1992, vol. 20, pp. 255–268.
27. Tauler, R., Izquierdo-Ridorsa, A., and Casassas, E., *Chemom. Intel. Lab. Systems*, 1993, vol. 18, pp. 293–300.
28. Juan, A. de, Van der Heyden, Y., Tauler, R., and Massart, D.L., *Anal. Chim. Acta*, 1997, vol. 346, no. 2, pp. 307–318.
29. Kudrev, A.G., *Koord. Khim.*, 1999, vol. 25, no. 2, pp. 152–159.

30. Gampp, H., Maeder, M., Meyer, C.J., and Zuberbuhler, A.D., *Talanta*, 1985, vol. 32, no. 12, pp. 1133–1139.

31. Gampp, H., Maeder, M., Meyer, C.J., and Zuberbuhler, A.D., *Talanta*, 1986, vol. 33, no. 12, pp. 943–951.

32. Hamilton, W.C., *Statistics in Physical Science*, New York: Roland, 1964.

33. Bresler, S.E., *Molekulyarnaya biologiya* (Molecular Biology), Leningrad: Nauka, 1973.

34. Vedenov, A.A., Dykhne, A.M., and Frank-Kamenetskii, M.D., *Usp. Fiz. Nauk*, 1971, vol. 105, no. 3, pp. 479–519.